Chain-length-dependent change in the structure of self-assembled monolayers of n-alkanethiols on Au(111) probed by broad-bandwidth sum frequency generation spectroscopy

AUTHOR(S):

Nishi, N; Hobara, D; Yamamoto, M; Kakiuchi, T

CITATION:

Nishi, N ...[et al]. Chain-length-dependent change in the structure of self-assembled monolayers of n-alkanethiols on Au(111) probed by broad-bandwidth sum frequency generation spectroscopy. JOURNAL OF CHEMICAL PHYSICS 2003, 118(4): 1904-1911

ISSUE DATE:

2003-01-22

URL:

http://hdl.handle.net/2433/39747

JOURNAL OF CHEMICAL PHYSICS VOLUME 118, NUMBER 4 22 JANUARY 2003

Chain-length-dependent change in the structure of self-assembled monolayers of *n*-alkanethiols on Au(111) probed by broad-bandwidth sum frequency generation spectroscopy

Naoya Nishi, Daisuke Hobara, Masahiro Yamamoto, and Takashi Kakiuchi[a)]
Department of Energy and Hydrocarbon Chemistry, Graduate School of Engineering, Kyoto University, Kyoto 606-8501, Japan

(Received 29 July 2002; accepted 29 October 2002)

The structure of the self-assembled monolayers (SAMs) of *n*-alkanethiols [$CH_3(CH_2)_nSH$, $n=3-11$, 13–15, 17] on Au(111) has been studied using broad-bandwidth sum frequency generation spectroscopy. Sum-frequency vibrational spectra show three pronounced CH_3 vibrational modes for all alkanethiol investigated, indicating that the commonly accepted picture that the alkyl chain for the long-chain alkanethiol SAMs has the all-*trans* conformation applies even to the short chain SAMs. The chain-length dependence of the ratio of the intensity for the CH_3 symmetric vibrational mode to that for the CH_3 asymmetric mode clearly shows the odd–even effect due to the difference in the direction of methyl group for SAMs with odd and even *n*, also supporting that the alkyl chain of SAMs has the all-*trans* conformation. An analysis of the vibrational intensities with respect to the angle between the main axis of the methyl group and the surface normal reveals that the structure of the alkanethiol SAMs gradually changes with *n*. © *2003 American Institute of Physics.*
[DOI: 10.1063/1.1531098]

I. INTRODUCTION

The structure of self-assembled monolayers (SAMs) of alkanethiols on gold has been studied using a number of methods such as vibrational spectroscopy [infrared (IR) and Raman],[1] diffraction (x-ray, electrons, and He atoms),[2–5] and scanning probe microscopy.[6] It has been demonstrated that the SAMs form highly oriented and densely packed film commensurate with the structure of a gold surface. However, there exist many intriguing features that await further explanation.

The structure of the SAMs is influenced by several factors such as the attractive force between alkyl chains, the adsorption site of Au(111) surface where an S atom makes a covalent Au–S bond, and the surface-S–C angle. For long chain alkanethiol SAMs on gold, the structure is known to resemble the crystal structure of bulk odd *n*-alkanes, suggesting that the van der Waals interaction between alkyl chains plays a important role in determining the structure.[5,7] On the other hand, with the decreases in *n* and in the van der Waals interaction, the structure is expected to become more flexible. Porter *et al.* found that alkanethiol SAMs with different chain length on gold fall into two groups at room temperature.[8] The number of methylene unit, *n*, separating the two groups was reported to be 5–11 by using several methods.[8] They concluded that in the longer chain length the SAMs are in a crystallinelike state and in the shorter the SAMs are in a disordered state, though the details on the structure were not obtained. Fenter *et al.* found that the tilt angle and tilt direction of the alkanethiol are different for the alkanethiols $n \leqslant 13$ and $n \geqslant 15$ due to the difference in the crystal structures by using grazing incidence x-ray diffraction (GIXD).[3] They also found that the temperature of phase transition for $n=11$ alkanethiol SAMs is 50 °C.[2] Recently, we found that there exists a sharp bend in the chain-length-dependence of the FWHM of the reductive peak for the electrochemical desorption of *n*-alkanethiols on Au(111) at $n=9$,[9] suggesting a possible phase transition. Despite the previous reports, it is still unclear how the structure of alkanethiol SAMs vary with the chain length.

IR spectroscopy has played a central role in determining the structure of SAMs on gold.[7,8,10–12] By comparing the intensities of the methylene vibrational modes of alkanethiol SAMs with those in the bulk phase, both the tilt angle from surface normal of the alkyl chain and the rotation angle around its main axis were determined. This method is suitable for long-chain alkanethiol SAMs. Although the methyl vibrational modes of the SAMs can be resolved even in the short-chain SAMs, no quantitative analysis has been made regarding the tilt and rotation angles.

Sum frequency generation (SFG) spectroscopy, which is one of the second-order nonlinear optical techniques, is a powerful tool to obtain vibrational spectra at the interface.[13,14] SFG is more sensitive to the orientation of the methyl group in alkanethiol SAMs than IR because SFG signal depends not only on $\cos^2\theta$ term but also on higher order terms such as $\cos^6\theta$,[15] where θ is the methyl angle, that is, the angle between the main axis of the methyl group and the surface normal. Furthermore, SFG is selective only to molecules adsorbed at interfaces because the second-order susceptibility becomes zero in the media with inversion symmetry under the electric dipole approximation.[16] Although the sensitivity to the orientation and the selectivity to molecules at interfaces can be utilized to infer the orientation of alkanethiol SAMs on gold,[17–19] its potential usefulness has not yet been fully exploited.

a)Author to whom correspondence should be addressed. Electronic mail: kakiuchi@scl.kyoto-u.ac.jp

Broad-bandwidth sum frequency generation (BBSFG) spectroscopy[20–22] used in the present work is a variation of SFG, where a spectrum with the bandwidth of fs IR pulses can be measured.[23–28] This advantage eliminates artifacts in the spectra resulting from the correction of IR pulse intensity and the alignment of the IR beam in varying IR wavelength, making BBSFG suitable to a precise analysis of the orientation of the SAMs.

In the present paper, we report the structure of *n*-alkanethiol SAMs on Au(111) studied using BBSFG spectroscopy by systematically changing the alkyl-chain length. The results of SFG spectroscopy will show the existence of odd–even effects in the wide range of the chain length and the gradual change in the structure with the decrease in *n*. The origin of the change in the structure depending on the chain length will be discussed in terms of the competitive interactions of the van der Waals interaction and Au–S interaction in determining the structure.

II. EXPERIMENT

A. Materials

n-alkanethiols [$CH_3(CH_2)_nSH$, $n=3-11$, 13–15, 17] were purchased from Aldrich ($n=3,9,14,17$), Tokyo Kasei ($n=4,6,7,10,13,15$), and Wako ($n=5,8,11$) and were used as received. The substrates with alkanethiol SAM on the Au(111) surface were prepared as described elsewhere.[9] Briefly, gold was vapor-evaporated to a freshly cleaved mica surface, which was subsequently annealed at 530 °C for 8 h. The formation of Au(111) terraces was confirmed by scanning tunneling microscopy. The substrate was then immersed into the 10^{-3} mol/L ethanol solution of alkanethiol for more than 24 h.

B. SFG system

Our system used for BBSFG measurements (Tokyo Instruments, Inc.) is similar to that described by Richter *et al.*[22] A Ti:sapphire regeneratively amplified laser system (CPA2001, Clark-MXR) producing pulses with the wavelength of 775 nm, the pulse width of 150 fs, the energy of 800 μJ/pulse, and the repetition of 1 kHz, was used. An optical parametric amplifier (IR-OPA, Clark-MXR) was pumped by the pulses from CPA2001, and it generated signal and idler pulses. At an $AgGaS_2$ crystal, different frequency mixing of the signal and the idler pulses occurred, and resulted in IR pulses with the central wavenumber of $\sim$2900 cm^{-1}. For visible pulses, approximately 10% of the energy before the pulse compressor in CPA2001 was taken out from another port. The bandwidth of the output pulses (duration—150 ps, bandwidth—6 nm, energy—200 μJ/pulse) was compressed by a custom-made bandwidth compressor using a grating to obtain narrow-bandwidth visible pulses (duration—10 ps, bandwidth—12 cm^{-1}, energy—2.5 μJ/pulse). The IR and visible beams were made coaxial using a dichroic mirror that reflected the visible light but transmitted the IR light. Both IR and visible pulses were introduced to the SAM on Au(111) surface at the incident angle of 60° and overlapped temporally and spatially. The energy for IR and visible pulses are 1.5 and 2.5 μJ/pulse at the sample and the bandwidth $\sim$200 and 12 cm^{-1}, respectively. All IR and visible pulses as well as analyzed sum-frequency (SF) light were *p*-polarized. The visible light was separated from the SF light using three dichroic mirrors. The SF light was dispersed by a Czerny–Turner-type monochromator (MS7504, SOLAR TII) and detected by a charge-coupled device (DU420-BV, Andor) cooled at −80 °C.

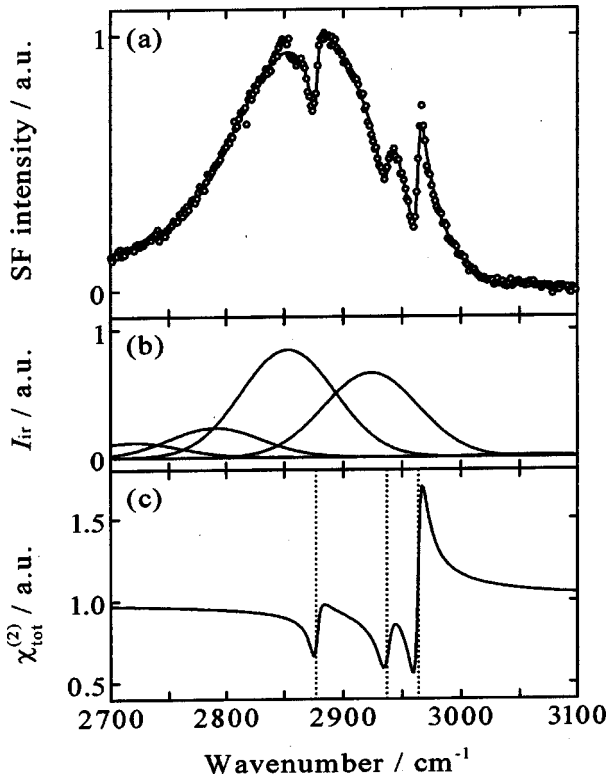

FIG. 1. (a) Sum-frequency vibrational spectra (open circle) for pentadecanethiol ($n=14$) SAM on Au(111) and fitted curves (full line) using Eq. (3); (b) decomposed broad-bandwidth IR pulses; and (c) the total second-order susceptibility, $\chi^{(2)}_{tot}$, normalized by $\chi^{(2)}_{NR}$. Dotted lines in (c) are 2877, 2937, 2964 cm^{-1}, respectively.

The substrates were rinsed with ethanol and dried in air for a few minutes before the measurements. SFG measurements for a sample was usually made within 40 min after taking out from the ethanol solution. We confirmed that the SF signals, both nonresonant and resonant components of the second-order susceptibility, were stable in this time scale. Typical time for the SFG signal acquisition was 5 min. The azimuthal angle dependence of the SF signal intensity showed that the intensity reached a maximum or a minimum every 60° turn.[29] The dependence indicates that the substrates have C_{3v} symmetry, proving that macroscopically the SAM-modified gold surface retains the symmetry property originated from Au(111) surface. All samples were measured at the azimuthal angle where the signal reached a maximum signal-to-noise ratio. All measurements were made at 22 ±1 °C.

III. RESULTS AND DISCUSSION

Figures 1(a) and 2(a) show the sum-frequency vibrational spectra for the pentadecanethiol (even *n*) and the

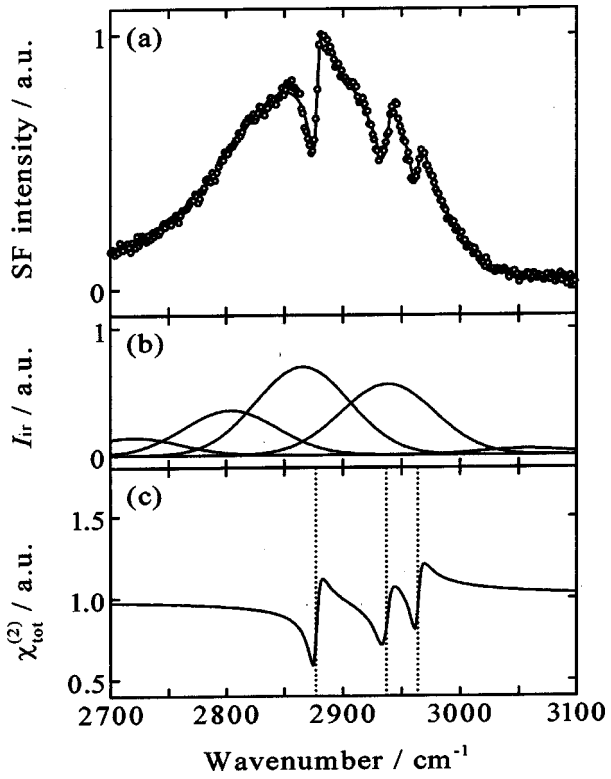

FIG. 2. (a) Sum-frequency vibrational spectra (open circle) for hexadecanethiol ($n=15$) SAM on Au(111) and fitted curves (full line) using Eq. (3); (b) decomposed broad-bandwidth IR pulses; and (c) the total second-order susceptibility, $\chi^{(2)}_{tot}$, normalized by $\chi^{(2)}_{NR}$. Dotted lines in (c) are 2877, 2937, 2964 cm^{-1}, respectively.

hexadecanethiol (odd n) SAMs on the Au(111) surface, respectively. All other spectra for SAMs with different alkyl-chain lengths for odd and even n we used were similar to Figs. 2(a) and 1(a), respectively. In each spectrum, one can see a broad-bandwidth envelope with three negative peaks having a narrow-bandwidth. The SF signal of the envelope can be assigned to the intraband transition of gold that causes the nonresonant component of the second-order susceptibility independent of the wavelength in the CH vibrational region.[30,31] The bandwidth of the envelope corresponds to that of IR pulses. The wavenumbers of the three negative peaks were 2877, 2937, and 2964 cm^{-1}, which can be assigned to the CH_3 symmetric vibrational mode (r^+), Fermi resonance between r^+ and the overtone of the CH_3 bending (r^+_{FR}), and CH_3 asymmetric vibrational mode (r^-), respectively.[22] The CH_2 symmetric and asymmetric vibrational modes, which should be observed at ~2850 and ~2920 cm^{-1}, respectively, in the IR spectroscopy,[8] could not be discerned in the spectra of all the n-alkanethiol SAMs studied. When the alkyl chain has all-*trans* conformation, it is known that the methylene vibrational modes does not appear in the sum-frequency spectra because of the inversion symmetry.[32] So far, the absence of the methylene vibrational modes has been confirmed for only long-chain ($n=15,17,21$) alkanethiol SAMs.[17,18,29,32–40] The absence of the signal at ~2850 and ~2920 cm^{-1} in the present results clearly indicates that the alkanethiol SAMs have all-*trans* conformation irrespective of the chain length.

To determine the magnitude of the vibrational intensities for the methyl vibrational modes of alkanethiol SAMs, a curve fitting method was employed using the following model.[18,29,37] The intensity of the SF light, I_{SF}, can be written as the product of the intensity of IR and visible pulses, I_{ir}, I_{vis}, and the square of the total second-order susceptibility of the interface, $\chi^{(2)}_{tot}$.[41]

$$I_{SF} \propto |\chi^{(2)}_{tot}|^2 I_{ir} I_{vis}. \tag{1}$$

The total susceptibility consists of the sum of the nonresonant component, $\chi^{(2)}_{NR}$, and the resonant components, $\chi^{(2)}_{R,\nu}$, for a vibrational mode, ν. Hence,

$$I_{SF} \propto \left| \chi^{(2)}_{NR} + \sum_{\nu} \chi^{(2)}_{R,\nu} e^{i\phi_\nu} \right|^2 I_{ir} I_{vis}, \tag{2}$$

where ϕ_ν represents the phase difference between $\chi^{(2)}_{NR}$ and $\chi^{(2)}_{R,\nu}$, both of which contain the Fresnel coefficients for SF, IR, and visible light.[41] Assuming that I_{ir} can be represented as the sum of Gaussian functions, I_{vis} as the delta function, $\chi^{(2)}_{NR}$ as constant, and $\chi^{(2)}_{R,\nu}$ as a Lorentzian function,[16,42] one may write the dependence of I_{SF} as a function of the angular frequency of IR, ω_{ir}, as

$$I_{SF}(\omega_{ir}) = \left| 1 + \sum_{\nu} \frac{A_\nu e^{i\phi_\nu}}{\omega_{ir} - \omega_\nu + i\Gamma_\nu} \right|^2 \times \left(\sum_n a_n \exp\left[-\frac{(\omega_{ir} - \omega_n)^2}{2\gamma_n^2} \right] \right), \tag{3}$$

where a_n, ω_n, and γ_n are the amplitude, the angular frequency, and the bandwidth of the n-th Gaussian function, respectively, and A_ν, ω_ν, and Γ_ν the amplitude, the angular frequency, and the bandwidth of the Lorentzian function for a vibrational mode, ν, respectively. It should be noted that A_ν is the amplitude normalized by $\chi^{(2)}_{NR}$.[37] The vibrational intensity of a mode, V_ν, may be defined as the ratio of the resonant component to the nonresonant component with $\omega_{ir} = \omega_\nu$, and thus represented as follows:

$$V_\nu \equiv \left| \frac{\chi^{(2)}_{R,\nu}(\omega_{ir} = \omega_\nu)}{\chi^{(2)}_{NR}} \right| = A_\nu / \Gamma_\nu. \tag{4}$$

The curves represented by Eq. (3) were fitted to the experimental data. From a preliminary fitting procedure, it was found to be acceptable in all spectra to fix the values of Γ_ν and ω_ν. The values of ω were fixed to be 2877, 2937, and 2964 cm^{-1}, and the values of Γ to be 4, 6, and 4 cm^{-1} for r^+, r^+_{FR}, and r^- modes, respectively. The value of γ was also fixed to 40 cm^{-1} because the envelope curves caused by broad-bandwidth IR pulses were reproducibly represented as the sum of the Gaussian function with the γ of 40 cm^{-1} at every ~70 cm^{-1} [Figs. 1(b) and 2(b)]. By using the FWHM of 94 cm^{-1} ($\sqrt{8 \ln 2} \times \gamma$) and the theoretical prediction where the product of the distribution of the time domain and the angular frequency domain ($\Delta t \, \Delta \omega$) is equal to 1.98 for a hyperbolic secant function,[43] the pulse width of IR pulses can be predicted to be 110 fs. The experimental value, 150 fs, is close but greater than the predicted value, suggesting that the pulses were slightly dispersed. The multi peaks may

be due to the multiple phase matching condition in the crystals. The remaining parameters in Eq. (3) were made variable in the curve fitting.

With these constraints, theoretical curves well reproduced the experimental data with three bands as shown in Figs. 1(a) and 2(a). The extracted susceptibilities containing the resonant components in Figs. 1(c) and 2(c) reveal that the three negative peaks in the spectra are not simply explained by the negative interference between the resonant and nonresonant components, and suggest the derivative shape due to ϕ_ν. The values of ϕ_ν are independent of both the difference in the modes and in the chain length (odd or even n) and determined to be 5.7 ± 0.3 rad. A small but nonnegligible deviation between the theoretical and experimental curves was found around $\sim 2855\ \mathrm{cm}^{-1}$ in all spectra. In this region, there are two possible bands that are ascribed to this deviation. One is the CH_2 symmetric vibrational mode (d^+) and the other is the CH_2 symmetric vibrational mode next to methyl group (d_ω^+) which is observed by some groups in the sum-frequency spectra.[37,40,44] Himmelhaus *et al.* reported that in the sum-frequency spectra of densely packed docosanethiol SAMs on polycrystalline gold, the d_ω^+ mode can be seen while the intensity of d^+ mode is not more than the noise level.[37] Thus, we assigned this small feature to the d_ω^+ mode. In the following, we will not use this small signature in the structural analysis because it is too small to be quantified.

The vibrational intensities, defined by Eq. (4), for r^+, r_{FR}^+, and r^- modes are shown in Figs. 3(a), 3(b), and 3(c), respectively. The values in Fig. 3 were averaged over 4–12 samples. Qualitatively, the intensities of r^+ and r_{FR}^+ modes are greater than the intensity of r^- mode in odd n, and smaller in even n. This feature is well known for the odd–even effect and agrees with the previous results of IR[45,46] and Raman spectroscopy.[47] The difference in the sum-frequency spectra for nonanethiol and decanethiol SAMs on gold was also reported.[18] Further, the chain-length dependence of the vibrational intensities shows that there exists a discrete change for even n between $n\leqslant 8$ and $n\geqslant 10$. For odd n, one can see the same feature between $n\leqslant 7$ and $n\geqslant 9$ though it is less prominent. Thus, it appears that there are two groups separated to the short one ($n\leqslant 8$) and long one ($n\geqslant 9$). Porter *et al.* found that the two groups exist for alkanethiol SAMs with a different chain length on gold at room temperature.[8] The number of the methylene unit separating the two groups was reported to be 5–11.[8] Also reported are $n=9$ from electrochemistry at room temperature,[9] and $n=11$ from GIXD at 50 °C,[2] supporting that the number separating two groups are $n\sim 9$ at room temperature.

Comparing the vibrational intensities obtained with theoretical predictions, we can estimate the orientation of the methyl group in the SAMs. To do so, the ratio of V_{r^-} to V_{r^+} was taken to eliminate the nonresonant component stemmed from a gold surface.[48] Using Eq. (4), the ratio is represented as

$$V_{r^-}/V_{r^+}=\left|\frac{\chi^{(2)}_{R,r^-}(\omega_{ir}=\omega_{r^-})}{\chi^{(2)}_{R,r^+}(\omega_{ir}=\omega_{r^+})}\right|. \tag{5}$$

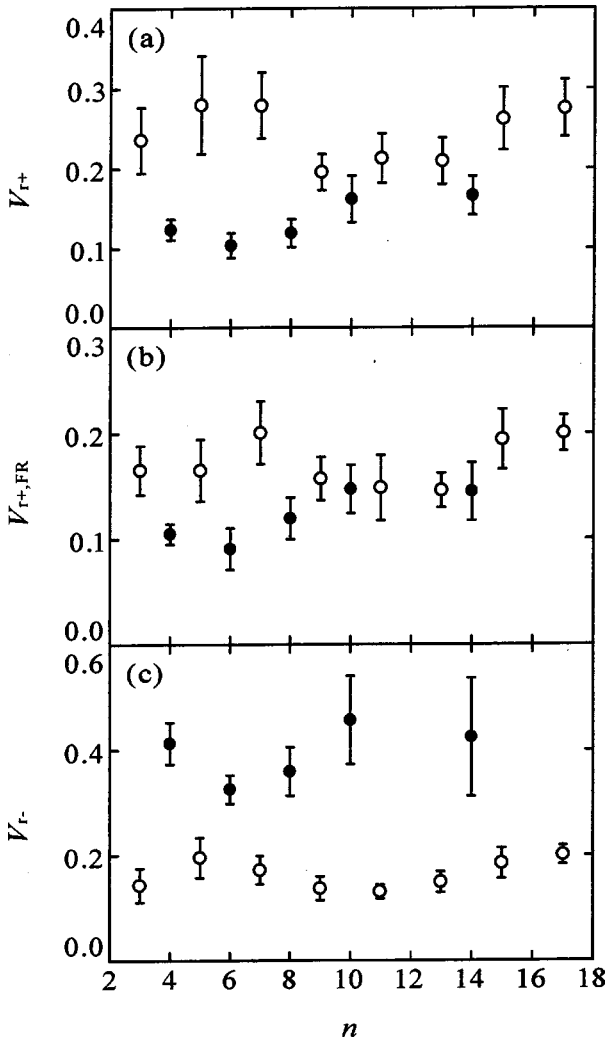

FIG. 3. Plots of the vibrational intensities for (a) r^+, (b) r_{FR}^+, and (c) r^- modes vs the number of the methylene unit of alkanethiol, n, for odd (open circle) and even (closed circle) numbers.

The resonant components of the susceptibilities caused by CH_3 vibrational modes can be derived using the transformation of the components of hyperpolarizabilities of a methyl group, β_{abc}, from the molecular system having an abc axis to the laboratory system having an xyz axis, and is represented by[42,49]

$$\chi^{(2)}_{R,\nu,ijk}=\frac{N_s}{\epsilon_0}\sum_{a,b,c}<T_{ia}T_{jb}T_{kc}>\beta_{abc}, \tag{6}$$

where N_s is the number of molecules at interfaces, ϵ_0 is the dielectric constant in vacuum, T_{ia}, T_{jb}, and T_{kc} are the ia, jb, and kc components of the transformation matrix of a vector from an abc axis to an xyz axis, respectively. The brackets represent the ensemble average over the orientational distribution. Here we define these orthogonal axes as follows: the z axis is the surface normal to the substrate, the x axis is parallel to the projection of the incident direction of the pulses to the surface, the c axis is the main axis of the methyl group parallel to the terminal C–C bond, and the a axis is parallel to the mirror plane of the methyl group assumed to have C_{3v} symmetry around the c axis. The sub-

script, ijk in $\chi^{(2)}_{\mathrm{R},\nu,ijk}$ means the contribution to the i component of the induced second-order polarization in response to the j and k components of the electric field of visible and IR pulses, on the surface. Given that the C_{6v} symmetry of the ensemble of the methyl groups, which reflects the symmetry of the first layer of Au(111) surface, and only the z component of the electric field of IR pulses being effective on the surface because of the surface selection rule, the nonvanishing components of all 27 components are xxz and zzz.

The transformation matrix in Eq. (6) was calculated to obtain the orientational dependence of $\chi^{(2)}_{\mathrm{R},\nu,ijk}$.[42,49] In the calculation, we took account of the C_{6v} symmetrical rotation of the methyl groups around the z axis. We also assumed that the alkyl chain rotates in two opposite directions with the same magnitude, that is, the two chain model.[5,7,45] The second-order susceptibilities for r^+ and r^- modes can then be represented in terms of the distribution of the methyl angle, θ, that is, the angle between z and c axes, as follows[48–50]

$$\chi^{(2)}_{\mathrm{R,r}^+,xxz}=\frac{N_s\beta_{ccc}}{8\epsilon_0}[\langle\cos\theta\rangle(7r+1)+\langle\cos 3\theta\rangle(r-1)], \tag{7}$$

$$\chi^{(2)}_{\mathrm{R,r}^+,zzz}=\frac{N_s\beta_{ccc}}{4\epsilon_0}[\langle\cos\theta\rangle(r+3)-\langle\cos 3\theta\rangle(r-1)], \tag{8}$$

$$\chi^{(2)}_{\mathrm{R,r}^-,xxz}=\frac{-1}{2}\chi^{(2)}_{\mathrm{R},r-,zzz}=\frac{-N_s(\beta_{aca}+\beta_{caa})}{8\epsilon_0}\langle\cos\theta-\cos 3\theta\rangle, \tag{9}$$

where $r=\beta_{aac}/\beta_{ccc}$. From Eq. (9), $\chi^{(2)}_{\mathrm{R},r^-}$ is proportional to $\langle\cos\theta-\cos 3\theta\rangle$, and when r is unity, from Eqs. (7) and (8), $\chi^{(2)}_{\mathrm{R},r+}$ is proportional to $\langle\cos\theta\rangle$ regardless of xxz or zzz. Then,

$$V_{\mathrm{r}^-}/V_{\mathrm{r}^+}=D\left(\frac{\langle\cos\theta-\cos 3\theta\rangle}{\langle\cos\theta\rangle}\right), \tag{10}$$

where D is a proportionality constant including the hyperpolarizabilities of a methyl group and the Fresnel coefficients. Using this equation, we can predict the tendency of the dependence of the ratio $V_{\mathrm{r}^-}/V_{\mathrm{r}^+}$ on the average orientation of the methyl groups. Although the exact value of r is not known, the values have been inferred to be in the range from 1.7 to 3.4.[51–56] If the value is greater than unity, the picture deduced below assuming that $r=1$ would remain to be the same at least qualitatively.

Figure 4 shows the dependence of $V_{\mathrm{r}^-}/V_{\mathrm{r}^+}$ on n. The distinctive difference in the values of $V_{\mathrm{r}^-}/V_{\mathrm{r}^+}$ for odd and even n can be seen: in the case of odd n the vibrational intensity for the r^+ mode is greater than that for the r^- mode, and *vice versa* in the case of even n. This feature again demonstrates the presence of the odd–even effect as in Fig. 3, but with higher clarity. The odd–even effect seen in the wide range of the chain length and the monotonous change

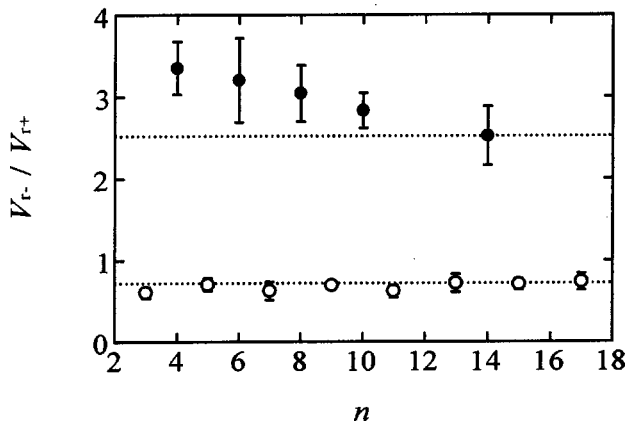

FIG. 4. Plots of the ratio of the vibrational intensity for the r^- mode to that for the r^+ mode, $V_{\mathrm{r}^-}/V_{\mathrm{r}^+}$, vs the number of methylene units of alkanethiol, n, for odd (open circle) and even (closed circle) numbers. Two dotted horizontal lines are the predicted values for long-chain alkanethiol SAMs (see the text for details).

in $V_{\mathrm{r}^-}/V_{\mathrm{r}^+}$ suggests that there is no dramatic change in the overall structure and in the ordering of alkanethiol SAMs with n.

Another interesting feature in Fig. 4 is the change in the ratio for even n while that for odd n is almost the same. With the decrease in even n, the ratio increases. For example, the ratio for $n=4$ is 33% greater than that for $n=14$. This feature should reflect the change in the average orientation of the methyl groups with n as represented in Eq. (10). When the phase-transition chain length $n=9$ at room temperature as mentioned in Fig. 3 is accounted, this change may begin around $n=9$ with the decrease in n due to the phase transition from an ordered phase to a less-ordered one. There are a few conceivable reasons that can bring in the change in the average orientation of the methyl groups. The most probable one is the change in the overall structure including the alkyl chain causing the change in the methyl angle, θ (Fig. 6, later). Second, the angular distribution of the methyl groups can vary with n because of the different rigidity of the SAMs. Third, a certain fraction of the alkanethiol molecules

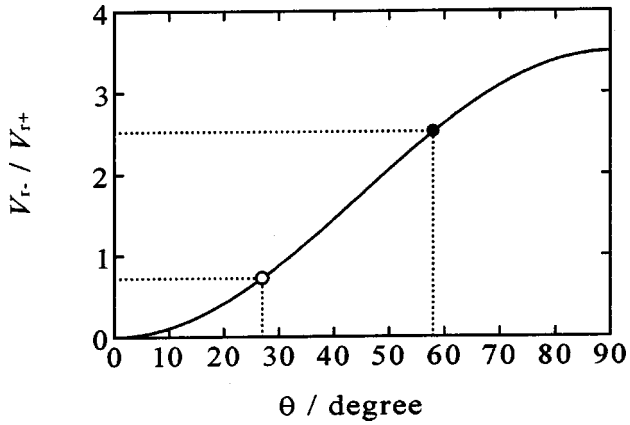

FIG. 5. Calculated curves of $V_{\mathrm{r}^-}/V_{\mathrm{r}^+}$ vs the methyl angle from surface normal, θ, when $D=3.5$. Two dotted vertical lines are 27° and 58° for odd and even n, respectively, predicted from 30° tilt and 50° rotation angles. Two horizontal lines are the values at 27° and 58°, respectively.

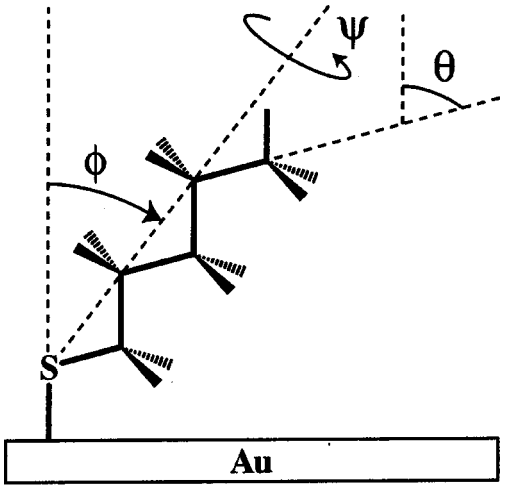

FIG. 6. A schematic view of the all-*trans* model. ϕ, ψ, and θ are the tilt angle of the alkyl chain with respect to the surface normal, the rotation angle around the main axis of the alkyl chain, and the methyl angle, respectively.

may take the *gauche* conformation at the terminal methylene unit depending on n,[57] despite the fact that the surface density of the methyl groups is the same in all SAMs studied. Other candidates such as the area of the domain size or the defects seem to be negligible. Hence we will consider the change in the ratio using Eq. (10), first, assuming only the overall structural change, and later taking account of the angular distribution of the methyl groups and the *gauche* conformation.

When there is no distribution of θ, the change in the ratio in Fig. 4 can be interpreted only in terms of the structural change with n. Figure 5 shows the predicted curve of $D\langle\cos\theta-\cos 3\theta\rangle/\langle\cos\theta\rangle$ $(=D\sin^2\theta)$ from Eq. (10). If the all-*trans* model is adopted, we can readily calculate the angle θ for odd and even n by using two parameters determining the structure; the tilt angle of the alkyl chain with respect to the surface normal, ϕ, and the rotation angle of the alkyl chain, ψ. The definitions of ϕ and ψ for the all-*trans* conformation are drawn in Fig. 6, where the S–C–C and C–C–C angles are assumed to be 110°. Preceding studies suggested that $\phi=30°$ and $\psi=50°$ for long-chain alkanethiol SAMs on Au(111).[3,4,8,11,45,58–65] The value of ψ may be a little greater than 45° which is assumed from an orthorhombic structure in the two chain model.[5,7] However, this difference does not influence the subsequent analysis. When $\phi=30°$ and $\psi=50°$, the values of θ in odd and even n are $\theta_{\mathrm{odd}}=27°$ and $\theta_{\mathrm{even}}=58°$, respectively. In Fig. 5 two vertical lines represent 27° and 58°, respectively. The predicted values are $0.21D$ and $0.72D$ in the case of odd (27°) and even (58°), respectively, whereas the experimental values of V_{r-}/V_{r+} are 0.71 and 2.5 for $n=15$ and 14, respectively. When D is assumed to be 3.5, the experimental and predicted values well agree with each other. Horizontal lines in Figs. 4 and 5 are the predicted values of the ratio when $D=3.5$, $\theta_{\mathrm{odd}}=27°$, and $\theta_{\mathrm{even}}=58°$. These two lines indicate that this simple prediction satisfactorily explains the overall structure of long-chain alkanethiol SAMs without assuming the presence of the angular distribution of methyl groups or the *gauche* conformation.

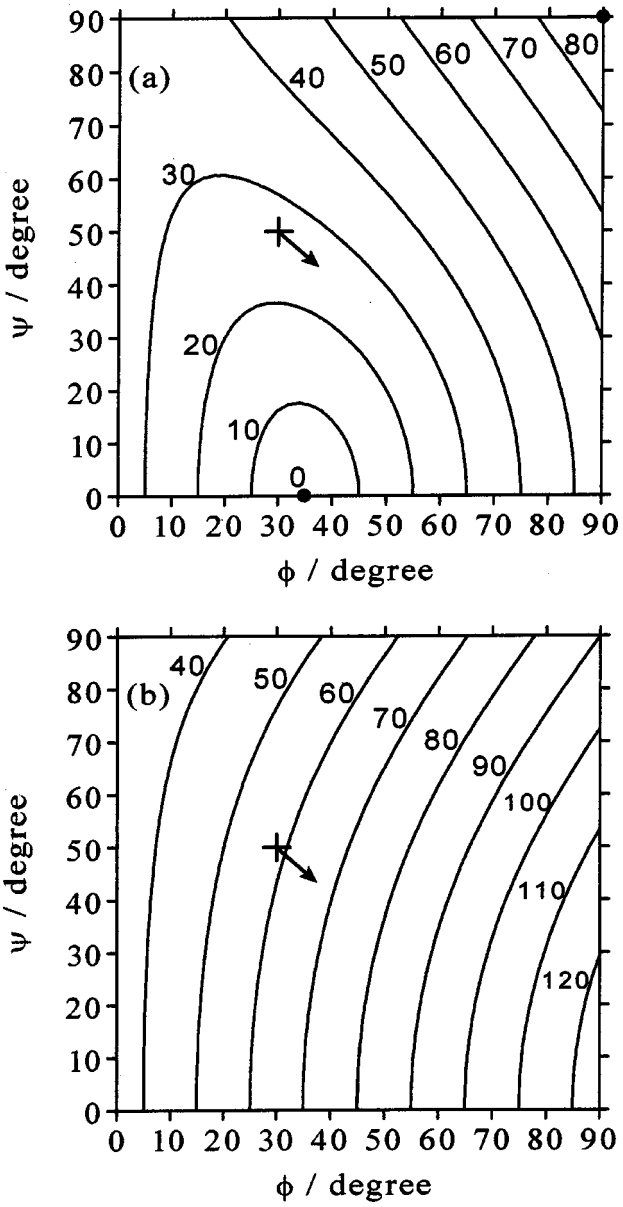

FIG. 7. Contour maps for (a) θ_{odd} and (b) θ_{even} as a function of the tilt angle, ϕ, and the rotation angle, ψ, calculated from the all-*trans* model. The crosses are the point of 30° tilt and 50° rotation angles. The arrows mean the direction along which the structure of the alkanethiol SAMs changes with a decrease in the chain length.

The change in the values in Fig. 4 can be interpreted using a theoretical curve in Fig. 5. The increase in the V_{r-}/V_{r+} for even n in the short-chain group reflects the increase in θ_{even} while odd n remains unchanged. From this tendency of the two angles, θ_{odd} and θ_{even}, we can recalculate the change in ϕ and ψ. Figures 7(a) and 7(b) show contours of θ_{odd} and θ_{even}, respectively, depending on ϕ and ψ in the all-*trans* model depicted in Fig. 6. In the contours, the direction along which the θ_{odd} remains invariant while θ_{even} becomes greater with the decrease in n is indicated as arrows toward the lower right. Here we assume that ϕ and ψ are independent no matter if n is odd or even. With the decrease in the chain length, ϕ becomes greater while ψ smaller. A structure with increased tilting with reducing n has been reported previously. The GIXD study reported by

Fenter *et al.* indicated that there are two groups for n; $n \leqslant 13$ and $n \geqslant 15$, where the structures of alkanethiol SAMs are different in terms of the tilt angle and the tilt direction.[3] Their results show that in the short-chain group the value of ϕ is 32°–34° while in the long-chain group the value is 30°–31°. The structure has also been shown in the near-edge x-ray absorption fine structure study; 37°–38° at $n=11$ and 33° at $n=15$.[57] Although the obtained values of ϕ depend on the methods used, the overall tendency is in good agreement with the present results.

We further consider two cases taking account of the distribution: one is the fraction of the *gauche* conformation at the terminal methylene unit, defined as α, and the other is the angular distribution of the methyl groups. Molecular dynamics studies[59,62,63,66] showed that the *gauche* conformation may exist at the terminal methylene unit in alkanethiol SAMs on Au(111) at 300 K. They suggested that α is at most several percent for long-chain alkanethiol SAMs ($n=12$,[63] 15[59,62,66]). This fraction of the *gauche* conformation is much lower than that of an isolated alkyl chain (2.9 kJ mol^{-1} higher than *trans* conformation[67]) probably because of the strong van der Waals interaction between alkyl chains. Indeed, our sum-frequency spectra do not show the feature of the chain defect which causes the d^+ mode, indicating that few alkanethiol molecules in the SAMs take the *gauche* conformation.

The distribution function, $f(\theta)$, for the *gauche* conformation at the terminal methylene unit can be written in the superposition form of three delta functions as

$$f(\theta)=(1-\alpha_{g1}-\alpha_{g2})\,\delta(\theta-\theta_0)+\alpha_{g1}\delta(\theta-\theta_{g1}) + \alpha_{g2}\delta(\theta-\theta_{g2}), \tag{11}$$

where θ_0 is the methyl angle for the all-*trans*, θ_{g1} and θ_{g2} are two methyl angles for the terminal *gauche*, and α_{g1} and α_{g2} are the fraction of θ_{g1} and θ_{g2}, respectively. Using the all-*trans* model with $\phi=30°$ and $\psi=50°$, θ_0, θ_{g1}, and θ_{g2} can be calculated to be 27°, 82°, and 119° for odd, and 58°, 97°, and 60° for even, respectively. Assuming that $\alpha_{g1}=\alpha_{g2}=\alpha$ and ϕ and ψ are invariant, the dependence of the ratio represented in Eq. (10) as a function of α was derived. Figure 8(a) shows the tendency of the ratio with the increase in α: for odd n, the ratio decreases while it slightly decreases for even. Since α is inferred to increase with the decrease in n,[57] the tendency shown in Fig. 8(a) does not clearly conform to the experimental one in Fig. 4.

With respect to the angular distribution of the methyl groups, the values of ϕ and ψ are expected to have distributions, causing the distribution in θ. The FWHM of the distribution of ϕ is reported to be 6° at 300 K in a molecular dynamics study.[63] The distribution of the methyl groups may be represented in the simple Gaussian form as

$$f(\theta)=\sin\theta\exp[-4\ln 2\times\{(\theta-\theta_0)/\Delta\theta\}^2], \tag{12}$$

where $\Delta\theta$ is the FWHM of the distribution of θ. Using this distribution function and Eq. (10), the dependence of the ratio as a function of $\Delta\theta$ was calculated, and is shown in Fig. 8(b). When considering the fact that the shorter the chain length the greater the distribution of the methyl groups due to the greater flexibility, the tendency in Fig. 8(b) is opposite to the experimental one in Fig. 4, i.e., for even n the ratio becomes smaller and for odd n greater with the increase in $\Delta\theta$. The discussion of the average orientation of the methyl groups is summarized as follows: both the presence of the *gauche* conformation and the distribution of the methyl groups are not likely to be major factors, indicating that the change in the experimental V_{r-}/V_{r+} is due to the change in ϕ and ψ.

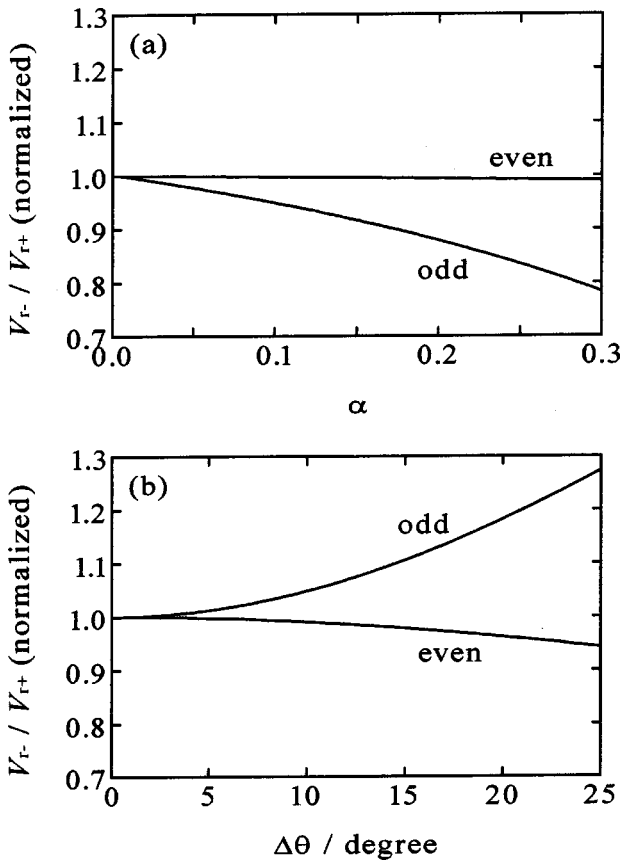

FIG. 8. The dependence of the calculated values of V_{r-}/V_{r+} (a) on the fraction of the *gauche* conformation, α, calculated from Eqs. (10) and (11), and (b) on the FWHM of the angular distribution of the methyl angle, $\Delta\theta$, calculated from Eqs. (10) and (12).

What remains to be explained is why the short chain alkanethiol SAMs prefer a more-tilted and less-rotated structure compared to the long chain. Presumably, with the decrease in n, the van der Waals interaction becomes weaker and the Au–S interaction, which affects surface-S–C angle, would mainly determine the orientation. In recent first-principles calculations, there are a few attempts to reveal the Au–S interaction in alkanethiol SAMs on Au(111) with $n=1$–3.[68,69] Further first-principles calculations that properly take account of the van der Waals interaction are required to elucidate the structure of SAMs with the short chain.

IV. CONCLUSIONS

The present BBSFG spectroscopy study of *n*-alkanethiol SAMs on Au(111) with systematically changing the alkyl-chain length demonstrates that the alkyl chain of the SAMs have the all-*trans* conformation regardless of n, and that the

structure of the SAMs varies with *n*, which is likely to be related to the phase transition. The analysis of the orientation of the methyl groups clearly show the structure changes toward more-tilted and less-rotated orientation with the decrease in *n*, which is likely to be due to the weaker van der Waals interaction in alkanethiol SAMs with the short chain.

The combination of BBSFG that provides reliable spectra with the theoretical analysis of the orientation is powerful to investigate the structure of SAMs consisting of different types of thiols such as aromatic-derivatized, alkoxy-derivatized, and fluorinated thiols, both *ex situ* and *in situ*.

ACKNOWLEDGMENTS

This work was partially supported by a Grant-in-Aid for Scientific Research (No.14205120) from the Ministry of Education, Science, Sports, and Culture, Japan, and CREST of JST (Japan Science and Technology). The SFG system employed in the present study is part of the IRPAF (Interfacial Reaction Properties Analysis Facilities) in Department of Energy and Hydrocarbon Chemistry, Graduate School of Engineering, Kyoto University.

[1] L. H. Dubois and R. G. Nuzzo, Annu. Rev. Phys. Chem. **43**, 437 (1992).
[2] P. Fenter, P. Eisenberger, and K. S. Liang, Phys. Rev. Lett. **70**, 2447 (1993).
[3] P. Fenter, A. Eberhardt, K. S. Liang, and P. Eisenberger, J. Chem. Phys. **106**, 1600 (1997).
[4] L. H. Dubois, B. R. Zegarski, and R. G. Nuzzo, J. Chem. Phys. **98**, 678 (1993).
[5] N. Camillone III, C. E. D. Chidsey, G. Liu, and G. Scoles, J. Chem. Phys. **98**, 3503 (1993).
[6] G. E. Poirier, Chem. Rev. **97**, 1117 (1997).
[7] R. G. Nuzzo, E. M. Korenic, and L. H. Dubois, J. Chem. Phys. **93**, 767 (1990).
[8] M. D. Porter, T. B. Bright, D. L. Allara, and C. E. D. Chidsey, J. Am. Chem. Soc. **109**, 3559 (1987).
[9] T. Kakiuchi, H. Usui, D. Hobara, and M. Yamamoto, Langmuir **18**, 5231 (2002).
[10] R. G. Nuzzo and D. L. Allara, J. Am. Chem. Soc. **105**, 4481 (1983).
[11] R. G. Nuzzo, L. H. Dubois, and D. L. Allara, J. Am. Chem. Soc. **112**, 558 (1990).
[12] P. E. Laibinis, R. G. Nuzzo, and G. M. Whitesides, J. Phys. Chem. **96**, 5097 (1992).
[13] X. D. Zhu, H. Suhr, and Y. R. Shen, Phys. Rev. B **35**, 3047 (1987).
[14] J. H. Hunt, P. Guyot-Sionnest, and Y. R. Shen, Chem. Phys. Lett. **133**, 189 (1987).
[15] C. Hirose, N. Akamatsu, and K. Domen, Appl. Spectrosc. **46**, 1051 (1992).
[16] Y. R. Shen, *The Principles of Nonlinear Optics* (Wiley, New York, 1984).
[17] R. N. Ward, P. B. Davies, and C. D. Bain, J. Phys. Chem. **97**, 7141 (1993).
[18] M. A. Hines, J. A. Todd, and P. Guyot-Sionnest, Langmuir **11**, 493 (1995).
[19] Y.-S. Shon, R. Colorado, C. T. Williams, C. D. Bain, and T. R. Lee, Langmuir **16**, 541 (2000).
[20] E. W. M. van der Ham, Q. H. F. Vrehen, and E. R. Eliel, Opt. Lett. **21**, 1448 (1996).
[21] E. W. M. van der Ham, Q. H. F. Vrehen, and E. R. Eliel, Surf. Sci. **368**, 96 (1996).
[22] L. J. Richter, T. P. Petralli-Mallow, and J. C. Stephenson, Opt. Lett. **23**, 1594 (1998).
[23] R. Braun, B. D. Casson, C. D. Bain, E. W. M. van der Ham, Q. H. F. Vrehen, E. R. Eliel, A. M. Briggs, and P. B. Davies, J. Chem. Phys. **110**, 4634 (1999).
[24] D. Star, T. Kikteva, and G. W. Leach, J. Chem. Phys. **111**, 14 (1999).
[25] M. Bonn, C. Hess, and M. Wolf, J. Chem. Phys. **115**, 7725 (2001).
[26] T. Ishibashi and H. Onishi, Chem. Phys. Lett. **346**, 413 (2001).
[27] K. A. Briggman, J. C. Stephenson, W. E. Wallace, and L. J. Richter, J. Phys. Chem. B **105**, 2785 (2001).
[28] E. L. Hommel, G. Ma, and H. C. Allen, Anal. Sci. **17**, 1325 (2001).
[29] M. S. Yeganeh, S. M. Dougal, R. S. Polizzotti, and P. Rabinowitz, Phys. Rev. Lett. **74**, 1811 (1995).
[30] E. A. Potterton and C. D. Bain, J. Electroanal. Chem. **409**, 109 (1996).
[31] A. Tadjeddine, A. Le Rille, O. Pluchery, F. Vidal, W. Q. Zheng, and A. Peremans, Phys. Status Solidi A **175**, 89 (1999).
[32] A. L. Harris, C. E. D. Chidsey, N. J. Levinos, and D. N. Loiacono, Chem. Phys. Lett. **141**, 350 (1987).
[33] C. D. Bain, P. B. Davies, T. H. Ong, R. N. Ward, and M. A. Brown, Langmuir **7**, 1563 (1991).
[34] T. H. Ong, P. B. Davies, and C. D. Bain, Langmuir **9**, 1836 (1993).
[35] Y. Tanaka, S. Lin, M. Aono, and T. Suzuki, Appl. Phys. B: Lasers Opt. **68**, 713 (1999).
[36] C. T. Williams, Y. Yang, and C. D. Bain, Langmuir **16**, 2343 (2000).
[37] M. Himmelhaus, F. Eisert, M. Buck, and M. Grunze, J. Phys. Chem. B **104**, 576 (2000).
[38] M. Zolk, F. Eisert, J. Pipper, S. Herrwerth, W. Eck, M. Buck, and M. Grunze, Langmuir **16**, 5849 (2000).
[39] M. Epple, A. M. Bittner, K. Kuhnke, K. Kern, W.-Q. Zheng, and A. Tadjeddine, Langmuir **18**, 773 (2002).
[40] B. C. Chow, T. T. Ehler, and T. E. Furtak, Appl. Phys. B: Lasers Opt. **74**, 395 (2002).
[41] C. D. Bain, J. Chem. Soc., Faraday Trans. **91**, 1281 (1995).
[42] P.-F. Brevet, *Surface Second Harmonic Generation* (Presses Polytechniques et Universitaires Romandes, Lausanne, 1997).
[43] C. Rulliére, *Femtosecond Laser Pulses* (Springer-Verlag, New York, 1998).
[44] S. R. Goates, D. A. Schofield, and C. D. Bain, Langmuir **15**, 1400 (1999).
[45] P. E. Laibinis, G. M. Whitesides, D. L. Allara, Y.-T. Tao, A. N. Parikh, and R. G. Nuzzo, J. Am. Chem. Soc. **113**, 7152 (1991).
[46] S.-C. Chang, I. Chao, and Y.-T. Tao, J. Am. Chem. Soc. **116**, 6792 (1994).
[47] M. A. Bryant and J. E. Pemberton, J. Am. Chem. Soc. **113**, 8284 (1991).
[48] M. S. Johal, E. W. Usadi, and P. B. Davies, J. Chem. Soc., Faraday Trans. **92**, 573 (1996).
[49] C. Hirose, N. Akamatsu, and K. Domen, J. Chem. Phys. **96**, 997 (1992).
[50] G. R. Bell, C. D. Bain, and R. N. Ward, J. Chem. Soc., Faraday Trans. **92**, 515 (1996).
[51] C. Hirose, H. Yamamoto, N. Akamatsu, and K. Domen, J. Phys. Chem. **97**, 10064 (1993).
[52] Y. R. Shen, in *Laser Spectroscopy and Photochemistry on Metal Surfaces*, edited by H.-L. Dai and W. Ho (World Scientific, Singapore, 1995), Chap. 1.
[53] K. Wolfrum and A. Laubereau, Chem. Phys. Lett. **228**, 83 (1994).
[54] D. Zhang, J. Gutow, and K. B. Eisenthal, J. Phys. Chem. **98**, 13729 (1994).
[55] R. Braun, B. D. Casson, and C. D. Bain, Chem. Phys. Lett. **245**, 326 (1995).
[56] R. Edgar, J. Y. Huang, R. Popovitz-Biro, K. Kjaer, W. G. Bouwman, P. B. Howes, J. Als-Nielsen, Y. R. Shen, M. Lahav, and L. Leiserowitz J. Phys. Chem. B **104**, 6843 (2000).
[57] D. Fischer, A. Marti, and G. Hähner, J. Vac. Sci. Technol. A **15**, 2173 (1997).
[58] A. Ulman, J. E. Eilers, and N. Tillman, Langmuir **5**, 1147 (1989).
[59] J. Hautman and M. L. Klein, J. Chem. Phys. **93**, 7483 (1990).
[60] M. M. Walczak, C. Chung, S. M. Stole, C. A. Widrig, and M. D. Porter, J. Am. Chem. Soc. **113**, 2370 (1991).
[61] P. Fenter, A. Eberhardt, and P. Eisenberger, Science **266**, 1216 (1994).
[62] W. Mar and M. L. Klein, Langmuir **10**, 188 (1994).
[63] R. Bhatia and B. J. Garrison, Langmuir **13**, 765 (1997).
[64] F. Balzer, R. Gerlach, G. Polanski, and H.-G. Rubahn, Chem. Phys. Lett. **274**, 145 (1997).
[65] H. U. Müller, M. Zharnikov, B. Völkel, A. Schertel, P. Harder, and M. Grunze, J. Phys. Chem. B **102**, 7949 (1998).
[66] J. Hautman and M. L. Klein, J. Chem. Phys. **91**, 4994 (1989).
[67] J.-P. Ryckaert and A. Bellemans, Faraday Discuss. Chem. Soc. **66**, 95 (1978).
[68] Y. Yourdshahyan and A. M. Rappe, J. Chem. Phys. **117**, 825 (2002).
[69] Y. Morikawa, T. Hayashi, C. C. Liew, and H. Nozoye, Surf. Sci. **507-510**, 46 (2002).